

Time-dependent luminescence of self-trapped excitons in alkaline-earth fluorides excited by femtosecond laser pulses

R. Lindner,¹ R. T. Williams,² and M. Reichling^{3,*}

¹*Fachbereich Physik, Freie Universität Berlin, Arnimallee 14, 14195 Berlin, Germany*

²*Department of Physics, Wake Forest University, Winston-Salem, North Carolina 27109*

³*Department Chemie, Universität München, Butenandtstraße 5-13, 81377 München, Germany*

(Received 22 February 2000; revised manuscript received 17 August 2000; published 30 January 2001)

We studied the decay of self-trapped excitons (STE's) in BaF₂, SrF₂, and CaF₂ excited at room temperature by two-photon absorption of femtosecond laser pulses by recording time-resolved triplet-luminescence spectra. For BaF₂ we detected significant spectral changes as a function of decay time but this effect was much less pronounced for SrF₂ and barely to be identified in CaF₂. A careful analysis of BaF₂ data revealed two principal decay times of 0.6 μs and approximately 4 μs, respectively, where the latter is actually a range of decay times correlating with photon energy within the luminescence band. We attribute this spectral characteristic to a superposition of contributions from several relaxed STE configurations while the two principal decay times are believed to result from the zero-field splitting of the ³Σ_u⁺ state of the STE.

DOI: 10.1103/PhysRevB.63.075110

PACS number(s): 78.47.+p; 78.55.Hx

I. INTRODUCTION

Intrinsic electron-hole recombination luminescence in the alkaline-earth fluorides BaF₂, SrF₂, and CaF₂ occurs via self-trapped exciton (STE) states characterized by substantial lattice relaxation. Singlet and triplet states of the STE are split by crystal-field interactions in the *C*_{1*h*} point symmetry of the relaxed lattice configurations. Neglecting crystal-field splitting for the moment in order to employ the more generic notation appropriate to *D*_{∞*h*} molecular symmetry, we will refer to the singlet and triplet excited states as ¹Σ_u⁺ and ³Σ_u⁺, which decay to the ¹Σ_g⁺ ground state by the emission of characteristic luminescence.¹ While the singlet-luminescence has a short lifetime of a few nanoseconds at low temperatures, the ³Σ_u⁺ state is metastable with typical decay times longer than microseconds. Only the triplet luminescence will be discussed here. It has been extensively studied by Williams *et al.*¹ who investigated the decay behavior after excitation with electron pulses. At 10 K they found that for all of the three materials there are three main decay constants ranging from about 50 μs to several milliseconds. A fourth component of 29 ms was found in BaF₂ only, but it was not investigated in detail. When raising the temperature, the three decay times merged into one around 50 K in CaF₂ and around 100 K in SrF₂, but there were also indications that it is possible to observe two components at higher temperatures. There is only one paper² known to us about the temperature dependence of the decay times for BaF₂ covering the temperature range from 5 to 160 K. As pointed out by Williams, *et al.*,¹ the different decay times of the STE's at low temperatures could originate either from different spatial configurations described below or from different transition probabilities of three triplet sublevels in the crystal field experienced by the STE, or from a combination of the two.

Generally, luminescence spectra of STE's in fluorides are very broad, asymmetric, and similar for BaF₂, SrF₂, and CaF₂ but one finds that the details of the spectra depend on experimental conditions.³⁻⁵ There are several reasons that

could account for the observed differences in shape and position of the luminescence spectra where the most trivial one is the characteristic of the spectral response of the experimental apparatus used. Furthermore, the sample temperature can be of influence.⁵ As we will demonstrate below, also the position and width of the sampling interval for the luminescence in a time-resolved measurement play an important role.

In the present paper we report on luminescence measurements performed at room temperature with spectral and time resolution, and revisit the question of different relaxed STE configurations and their effect on the luminescence. We believe that a key to their understanding is an investigation of the detailed spectral features of the luminescence spectra, correlated with time dependence. The availability of intense ultrashort laser pulses in the ultraviolet spectral region now allows us to study the dynamics of excitons also in wide-band-gap halides.⁶ In this paper we present luminescence spectra of STEs generated in fluorides with femtosecond ultraviolet laser pulses that we probe with an optical multi-channel analyzer having gated time resolution. We present a comparative study of the three alkaline-earth fluorides, BaF₂, SrF₂, and CaF₂, and demonstrate that they differ significantly with respect to spectral features of their time-dependent luminescence decay. In accordance with the mentioned previous studies where STEs have been created by pulsed electron irradiation, we observe more than one decay time but additionally find a spectral variation of the largest decay time for BaF₂. Our data can consistently be interpreted in terms of a model proposing that the levels of several STE configurations are occupied at room temperature and that the temporal and spectral behavior of the luminescence decay is governed by the specific decay times for the configurations or transformations from one configuration into another.

II. EXPERIMENT

Samples were the highest purity BaF₂, SrF₂, and CaF₂ single crystals grown by Korth (Kiel, Germany) with cleaved

or polished (111) surfaces. Sample thickness varied but was typically 5 mm. To generate the light for excitation, a multiline Ar⁺ laser (Spectra-Physics, Mountain View, USA) pumped a mode-locked Ti:sapphire laser (CDP, Moscow, Russia) which seeded a regenerative amplifier (Positive Light, Los Gatos, USA) pumped by a frequency-doubled Nd:YAG (where YAG stands for yttrium aluminum garnet) laser (Spectra-Physics, Mountain View, USA) radiation. The unit provided pulses with a length of typically 130 fs and an energy of up to 2 mJ at 10-Hz repetition rate. The fundamental beam with a wavelength of 840 nm was frequency doubled two times by BBO crystals where the fourth harmonic was separated from the fundamental and the second harmonic by several dielectric mirrors in the optical path. By this procedure we generated laser pulses with 5.9-eV photon energy and 10- μ J pulse energy and a pulse width of less than 270 fs. The pulse energy of the fourth-harmonic pulses could be reduced in a controlled way by a small misalignment of the phase-matching angle of the second BBO crystal. Due to the high nonlinearity in ultraviolet pulse generation, instabilities in the fundamental light intensity are strongly amplified and are the main source of fluctuations in the intensity of the exciting beam. Due to these nonlinearities and fluctuations introduced by the Nd:YAG laser, the fourth-harmonic pulses had a rms intensity noise of typically 10%, although the Ti:sapphire laser exhibited excellent stability. By performing signal averaging and normalization as described below we could, however, obtain a much better signal-to-noise ratio in our measurements.

Samples were irradiated with the unfocused beam of 3-mm diameter providing a maximum photon density of $1.5 \times 10^{14} \text{ cm}^{-3}$. In our experiments, STEs were excited via a two-photon process. As the two-photon cross section can be assumed to be small, we can anticipate that the actual excitation density was orders of magnitudes smaller than the photon density and we can therefore exclude that our measurements were affected by an interaction between excitons, as has been observed in high excitation density experiments.^{7,8} With our excitation we solely reach excitonic states or states just above the conduction-band edge, so we can also exclude multiple excitation effects as observed when exciting with synchrotron radiation.⁹

To detect the luminescence we used a gated optical multichannel analyzer system (Princeton Instruments, Trenton, USA) consisting of a grating monochromator (150 groves/mm, blazed at 500 nm) with an overall spectral resolution of 4 nm and a delay generator (Stanford Research, Sunnyvale USA). The gate width could be adjusted between 20 ns and 3 μ s. Spectral light intensity was measured with an array of charge-coupled devices (CCD) where the dark current of each pixel was determined and used for background subtraction prior to each series of measurements. Nevertheless, the dark current turned out to be a severe limitation for our experiments since its intensity varied as a function of time and experimental history and in regions of low light intensity exceeded the measured signal by up to one order of magnitude. Consequently, we cannot exclude that the offset present in some of our time-dependent measurements is due to the dark current. The luminescence was sampled by a fused

silica lens with 20-mm focal length and guided through a fused silica glass fiber bundle to the entrance slit of the monochromator. We have not calibrated the wavelength-dependent transmission of the optical detection system, which is influenced by the transmission of the optical fiber and the characteristic of the focusing lens, the mirrors in the monochromator, and the CCD. Before each measurement, however, the monochromator was calibrated with respect to wavelength by a mercury lamp.

To improve the signal-to-noise ratio, we averaged the luminescence intensities of many laser shots. The measurements of the pulse energy dependence of the total luminescence intensity were done with a gate width of 2.5 μ s, a delay time of 30 ns, and an accumulation of 1000 shots; the luminescence decay measurements at early times with a gate width of 100 ns and an accumulation of 3000 shots; and the measurements at late times with a gate width of 1 μ s and an accumulation of 2000 shots, respectively. Fluctuations of the exciting pulse energy were compensated by dividing measured luminescence intensities by normalization factors. These factors were determined by a procedure where we first averaged exciting pulse energies before and after the respective measurement. From both averages we then derived a mean value. Finally this value was exponentiated with an exponential order determined by an independent measurement of the excitation pulse energy dependence of the respective material described in Sec. III. All measurements were performed at room temperature. The gate delay time was always set to at least 8 ns. Therefore, we can be sure to have observed only triplet-luminescence since the decay time of the singlet-luminescence is 10 ns at 10 K and certainly much shorter at room temperature.¹

III. RESULTS

In a first set of experiments we verified that we were able to cross the band gap under our excitation conditions and excluded that we were addressing only defect states in the band gap linearly absorbing the ultraviolet laser light. To accomplish this, we measured the STE luminescence as a function of the exciting laser pulse energy and compiled data for all investigated fluorides in Fig. 1. For a nonresonant two-photon absorption process in a double-logarithmic plot of luminescence intensity against pulse energy one would expect a slope of exactly two. In the case of BaF₂ we find this value within the error of the measurement. However, SrF₂ and CaF₂ exhibit some deviations. We conclude that we indeed observe two-photon absorption and deviations of the slopes from the value of two arise from processes related to impurities, structural imperfections, and surface preparation as has recently been suggested by Tsujibayashi *et al.*¹⁰ based on two-photon excited STE luminescence assisted by synchrotron radiation.

Luminescence spectra as obtained from BaF₂, SrF₂, and CaF₂ are displayed in Fig. 2 where the maxima have been normalized to unity for a better comparison. Spectra in the upper frame were obtained by integration of the spectral luminescence intensity over the time interval from 50 to 150 ns after excitation while measurements in the lower frame cov-

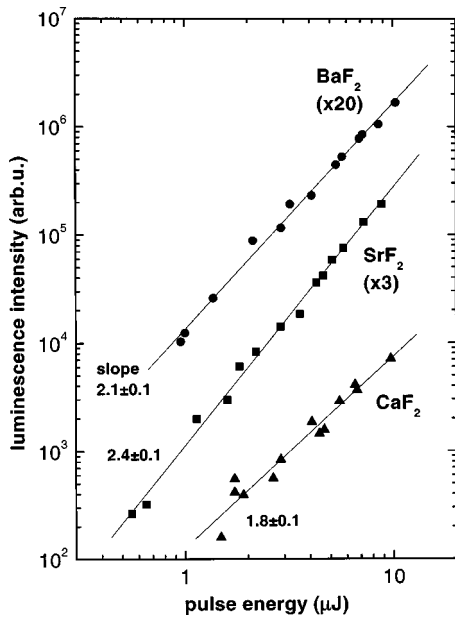


FIG. 1. Time-integrated luminescence intensities for BaF_2 , SrF_2 , and CaF_2 plotted as a function for the exciting laser-pulse energy E . The exponential order b for the STE excitation has been determined by fitting power functions $I(E) = aE^b$ to the data and we determined b values 2.1 ± 0.1 , 2.4 ± 0.1 , and 1.8 ± 0.1 for BaF_2 , SrF_2 , and CaF_2 , respectively.

ered the interval from 3 to 9 μs , respectively. The most obvious feature in Fig. 2 is the systematic variation of the maximum and width of the luminescence peaks within the series of investigated materials. The broadest and most redshifted luminescence peak is found for BaF_2 , while SrF_2 is the intermediate case, and CaF_2 exhibits the narrowest spectrum with a peak at the highest photon energy. On the one hand, we note that this trend follows the band-gap energies of the materials of 10.7, 10.9, and 11.5 eV, respectively.¹¹ It is expected that the exciton luminescence energy should scale approximately with the band gap in a family of otherwise similar materials. To understand the trend of luminescence bandwidths, however, it may also be helpful to note that increasing widths can be correlated with increasing the lattice constant as well as decreasing the band gap in this material family. The observation of a trend in increasing the STE luminescence bandwidth suggests that the degree of lattice relaxation in the STE depends significantly on the lattice constant, i.e., on the space available for the motion of the interstitial fluorine atom and the size of the vacancy binding the electron.

The second important observation is that the spectral shape of the luminescence peaks significantly depends on the delay between the excitation and the sampling interval. The effect is remarkably large in the case of BaF_2 where the emission maximum shifts from 4.4 eV at early times to 3.8 eV at late times and changes its shape completely. To describe this effect more clearly and somewhat quantitatively we calculated the centers of gravity of the spectra and displayed the corresponding data in Fig. 3. When applying this procedure, the intensity in the flanks of the luminescence peaks is strongly weighted and it becomes obvious that there

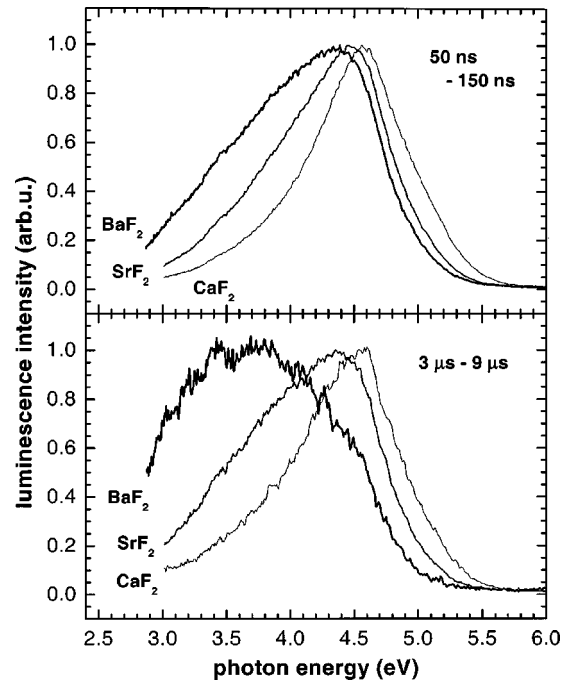


FIG. 2. STE luminescence spectra of BaF_2 , SrF_2 , and CaF_2 after excitation with femtosecond laser pulses of 5.9 eV photon energy. The plots show the luminescence yield integrated over time ranges from 50 to 150 ns and from 3 to 9 μs after excitation, respectively. The gate width was set to 100 ns for early times and 1 μs for late times. The maxima of all spectra are normalized to 1 for a better comparison.

is a shift for all three fluorides. This was not immediately evident for CaF_2 when comparing frames in Fig. 2 only. Figure 3 clearly represents the systematic trend in the progression from BaF_2 to CaF_2 and reveals that the shift in the center of gravity is nearly three times larger for the former than for the latter material. More quantitative information can, however, not be drawn from this figure since the numbers shown might be slightly affected by the reduced light

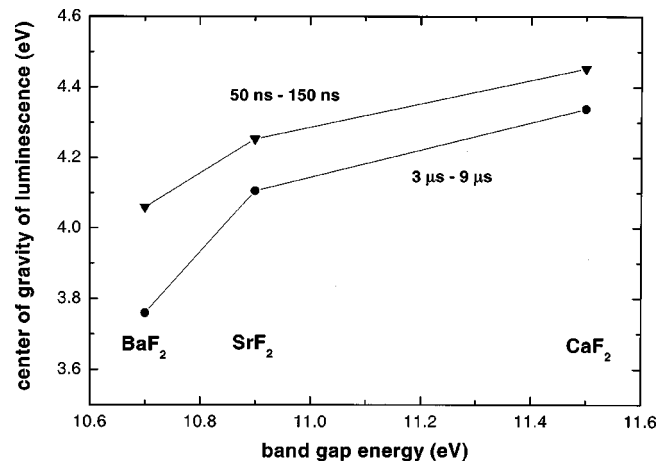


FIG. 3. Center of gravity of luminescence spectra in Fig. 2 plotted against the band-gap energies of the respective materials taken from Ref. 11.

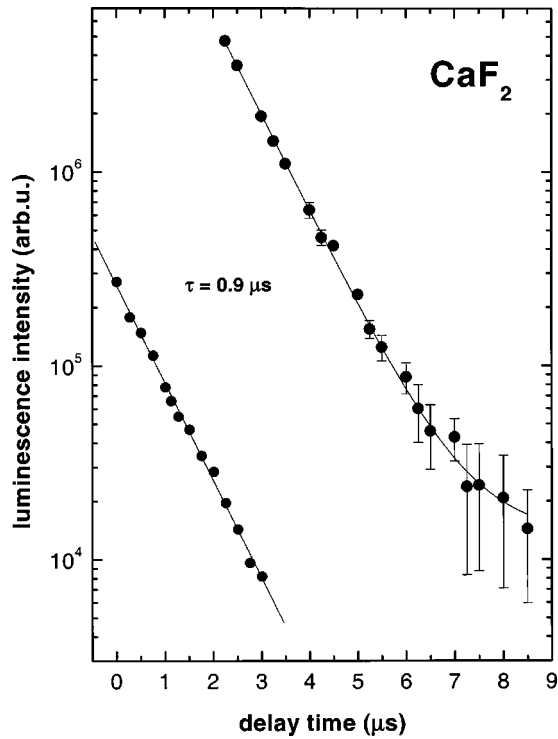


FIG. 4. Decay of the STE luminescence in CaF_2 at early and late delay times. Data points represent time-integrated luminescence spectra that were taken with a gate width of 100 ns and 1 μs for early and late times, respectively. Fits were done using a single exponential function with decay time τ ; however, for long delay times an additive constant is required to obtain a reasonably good fit.

transmission of our measurement system in the ultraviolet spectral region.

To investigate the temporal wavelength dependence of the luminescence in more detail we measured the decay times of the STE luminescence for all three fluorides and made an attempt to sample luminescence intensity only in selected spectral regions. In the case of SrF_2 and CaF_2 , however, spectral effects were too small to be extracted from the background at late delay times where spectral luminescence intensities are extremely small. Therefore, in Figs. 4 and 5 we show the decay of the luminescence when integrated over the entire spectrum and extract decay time constants of $(1.02 \pm 0.05) \mu\text{s}$ and $(0.86 \pm 0.05) \mu\text{s}$ for SrF_2 and CaF_2 , respectively. For very long delay times there are indications of an additional larger time constant; however, this cannot be separated unambiguously from a possible dark current background. In the case of BaF_2 we see spectral differences in the luminescence decay. Figure 6 shows time integrated spectra of several stages of the STE decay. For better comparison, spectra were normalized to unity and smoothed by averaging seven neighboring data points thus reducing the total number of measurements per curve from 474 to 68 points represented in the plots. It is obvious from Fig. 6 that the high-energy side of the spectra diminishes as a function of gate delay time while the low-energy side gains intensity.

To describe this effect quantitatively we have taken spectra for various delay times ranging from 1 to 20 μs and fitted

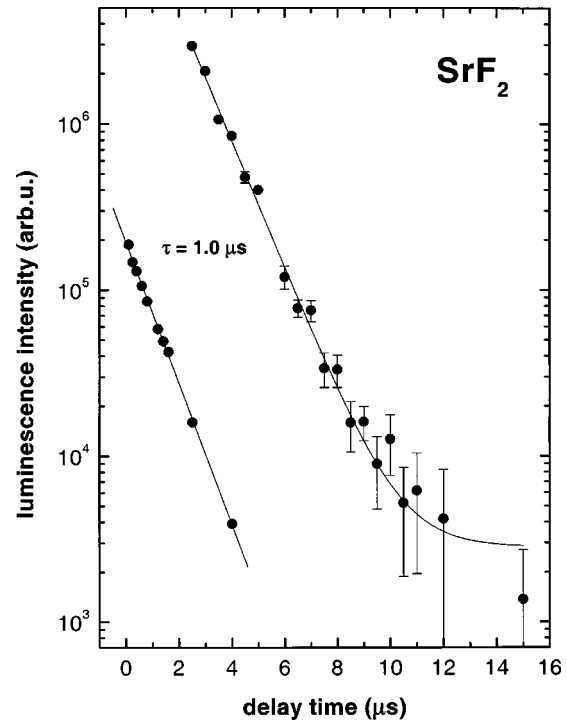


FIG. 5. Same data and evaluation as in Fig. 4 but for measurements on SrF_2 .

one spectrum with five Gaussian functions where four of them (see the inset of Fig. 7) shall represent the four different STE configurations postulated by Williams *et al.*¹ while the fifth accounts for the second-order intensity of the grating. The Gaussians obtained from the fit to this one spectrum were taken as templates also for the analysis of all other spectra. The delay time-dependent luminescence data shown in Fig. 7 has been obtained by integrating the spectral intensity over the photon energy range corresponding to the half width of each of the template Gaussians. Independent from the spectral behavior, we detected two principal decay constants, i.e., one more than in the case of SrF_2 and CaF_2 and

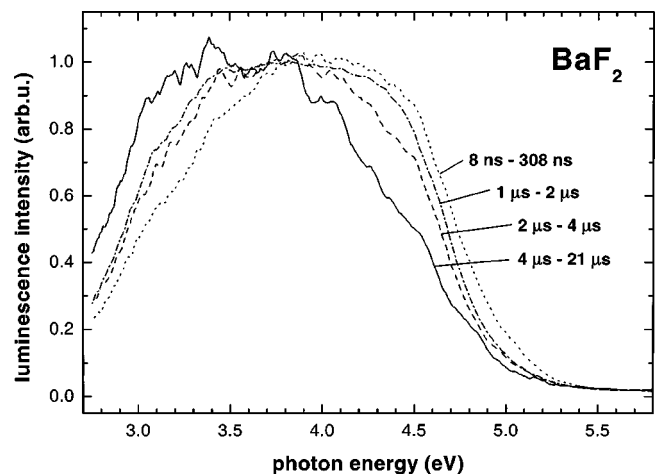


FIG. 6. Luminescence spectra of BaF_2 obtained by integration of the luminescence intensity over different time intervals. Spectra have been normalized to unity for a better comparison.

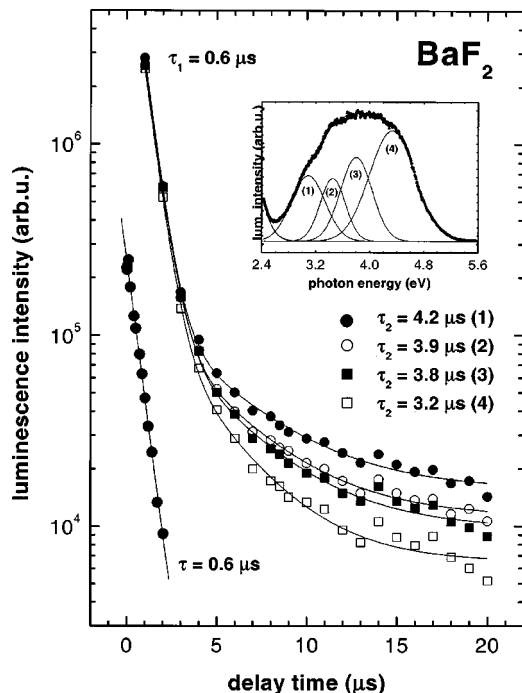


FIG. 7. The decay behavior of STE luminescence in BaF_2 . Data points at early delay times have been obtained with a gate width of 100 ns and by integration over the entire accessible spectrum. A fit of a single exponential function to the data yields a decay constant of $0.6 \mu\text{s}$. Late time luminescence data is displayed in four sets of data obtained by integrating luminescence intensity over four spectral regions defined by the FWHM of fitting Gaussian functions to the luminescence spectrum (delay 18 ns, gate width 350 ns) shown in the inset.

the fits also suggests a third time constant that is, however, again indiscernible from the background. At early times the decay is dominated by a uniform decay constant of $(0.60 \pm 0.05) \mu\text{s}$ while the curves split up into branches at later times. For the selected spectral regions we determined time constants of $(4.2 \pm 0.4) \mu\text{s}$, $(3.9 \pm 0.4) \mu\text{s}$, $(3.8 \pm 0.4) \mu\text{s}$, and $(3.2 \pm 0.3) \mu\text{s}$, respectively. Due to the overlap of integrated ranges of luminescence and the limited signal-to-noise ratio, this type of data analysis does not allow a precise determination of a time constant for a specific wavelength but yields the general spectral trend. The fact that two intermediate decay times are very close to each other, however, strongly suggests that the luminescence decay is indeed governed by three independent time constants. As displayed in Fig. 8 it is possible to very well fit the luminescence spectrum in the inset of Fig. 7 with only three Gaussians.

IV. DISCUSSION

The structure of the relaxed STE in the fluorite crystal and its possible configurations have been revealed by Call *et al.*¹² and Williams *et al.*¹ and are illustrated in Fig. 9. The STE is composed of a F_2^- molecular ion oriented in a $[111]$ direction^{13,14} commonly referred to as the H center part, and at the F center part there is an electron occupying a vacant F^- site. The possible configurations differ by the relative

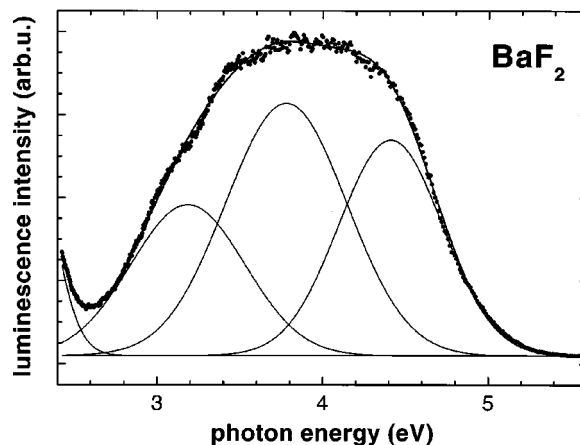


FIG. 8. Fit of three Gaussian functions to the luminescence spectrum shown in the inset of Fig. 7.

positions of the F and H center parts with respect to each other. The most plausible structure is configuration II which is formed by the dynamic process of STE formation without any additional ionic rearrangement.¹⁵ The question of the spatial configurations of the STE in alkaline-earth fluorides has been addressed by experimental¹⁶ and theoretical^{17,18} work. Adair *et al.*¹⁹ calculated total lattice energies for the configurations in SrF_2 and CaF_2 at zero temperature and found that all four configurations in both crystals have similar energies around 7.6 and 9.0 eV, respectively. In CaF_2 configuration II is a little lower than the others while in SrF_2 energies for configurations II and III do not differ from each other. Theoretical predictions on BaF_2 have, however, not been reported to the best of our knowledge. Experimental evidence pointing to the existence of different STE configurations has been presented by Eshita *et al.*,¹⁶ who measured STE absorption spectra of SrF_2 and observed two spectral subbands for the F center as well as the H center absorption differing in their decay times. In double-excitation measurements they also demonstrated that it is possible to transform one component into another.

Based on this knowledge we now develop the interpreta-

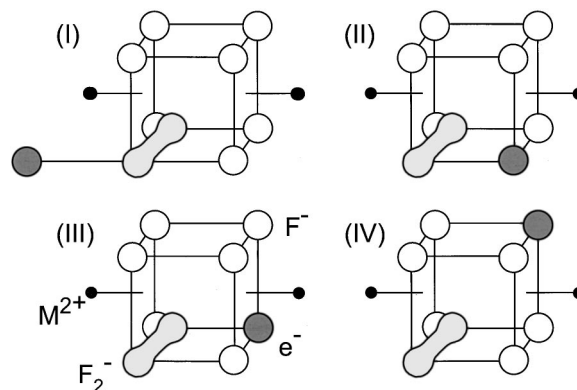


FIG. 9. Configurations of the self-trapped exciton as proposed by Williams *et al.* (Ref. 1) in their notations I, II, III, and IV. Alkaline-earth ions, fluorine ions, H centers, and F centers are represented by the symbols M^{2+} , F^- , F_2^- , and e^- , respectively.

tion of our time and spectrally resolved luminescence data. While the basic structure of the STE is the same for all materials investigated here, the dynamics of STE formation and occupation probability for certain configurations may be different since the ionic radii and lattice constants differ from each other. Barium has the largest ionic radius amounting to 129 picometer (pm) in contrast to 110 and 94 pm of strontium and calcium, respectively, and is comparable to that of the fluorine ion which is the largest species with 133 pm radius.²⁰ Due to the large space consumption of the cations, the unit cell of BaF₂ is larger than those of SrF₂ and CaF₂ and the lattice constants are 620, 580, and 546 pm, respectively.²¹ Therefore, the *H* center part of the STE has more space in the fluorine cage of BaF₂ than in the other fluorides which may result in a different STE formation dynamics and possibly more configurations that may become occupied. After the primary creation of an electron-hole pair in the form of a V_k center and an electron, the STE is formed by a combined rotational and translational movement of the F₂⁻ molecule from the [100] direction into the [111] direction driven by the excited electron filling the fluorine vacancy.¹⁵ This process naturally yields a STE with configuration II. Due to the large space available in BaF₂ it seems possible that a thermally excited neighboring F⁻ ion moves in the direction of the unoccupied lattice position and the electron localizes on the free next-neighbor ionic position, a process resulting in configuration III. In the case of configuration IV, two movements of F⁻ ions are necessary what appears to be a less probable case. The existence of this configuration has also been questioned by electron-spin resonance results¹² because the measured zero-field parameter *E* is too large for the expected vanishing of *E* on account of configuration IV states symmetry.¹ We anticipate that this configuration does not play any role in our measurements. Configuration I can be formed without movements of a F⁻ ion, but the way for rotating and translating the F₂⁻ molecule is longer than in configuration II. Therefore the occupation of configuration I is less probable than the occupation of configurations II and III, but all three of them can be observed in accordance with our observations for all investigated fluorides.

In our measurements on BaF₂ we find two time constants for the STE luminescence decay, one more than for the other fluorides. With a much higher density pulsed electron excitation of samples kept at a temperature of 10 K, Williams *et al.*¹ also determined one more decay constant for the triplet luminescence in BaF₂, in detail four, but only three for SrF₂ and CaF₂, respectively. They also measured a temperature dependence for SrF₂ and CaF₂. With increasing temperature the decay develops faster and the number of decay times reduces. This is also expected for BaF₂. At room temperature they measured two decay constants for SrF₂ and CaF₂. The shorter decay times 3 and 1.6 μs of SrF₂ and CaF₂, respectively, have the same order of magnitude as our values but are somewhat larger. We speculate that the deviations may be caused by different excitation methods of STE's where our low density multiphoton excitation might preferentially create STE's adjacent to defect sites resulting in a reduction of the STE lifetime. We propose that the two principal decay times are not related to the different STE

configurations but are a result of the splitting of the STE state into sublevels due to hyperfine and crystal-field interactions.

On the other hand, our data clearly shows a spectral characteristic in the STE luminescence decay behavior for BaF₂ in the form of a splitting of the larger luminescence time constant into three branches when analyzed with spectral resolution. We interpret this in terms of observing STEs in different configurations differing from each other in both their lifetime and the Stokes-shift of their recombination luminescence. For configuration II where *F* and *H* center parts are nearest neighbors, the lifetime and Stokes shift are the smallest but they increase with increasing distance between the defect centers, i.e., in the progression of configurations II, III, and I. This is well in accordance with the expectation for Franck-Condon transitions within such a molecular system in a halide crystal.^{22,23} We propose that in the case of BaF₂ at room temperature the levels corresponding to configurations II, III, and I are occupied yielding the relatively broad spectra shown in Fig. 2. The relations described above principally also hold for SrF₂ and CaF₂. We anticipate, however, that the occupation probability for the different STE configuration states critically depends on the ionic radii determining the steric properties of the fluorite unit cell for the respective material. For SrF₂ and CaF₂ the room-temperature occupation probability for configurations I and III is much smaller than that of configuration II due to the steric constraints imposed by the smaller lattice constants. Consequently, luminescence spectra are narrower for these materials and less redshifted than for BaF₂. In the case of CaF₂ we almost exclusively observe the recombination luminescence of type-II STEs.

V. CONCLUSIONS

In summary we have shown that the decay of self-trapped exciton luminescence in BaF₂ is distinctly different from that found for the other alkaline-earth halides. The analysis of spectrally resolved luminescence decay data suggests that for BaF₂ we are able to separate luminescence contributions from the decay of different STE configurations. The assumption of occupying STE configurations in BaF₂ but to a much lesser extent in SrF₂ and CaF₂ appears to be plausible when considering the different steric properties of the investigated materials. It remains an open question, however, whether the different configurations are occupied during the first few picoseconds of STE formation or later by thermal excitation. This question might be answered by time-resolved spectroscopic studies measuring transient light absorption by STE's that are currently in progress in our laboratory.

ACKNOWLEDGMENTS

The authors are grateful to M. Kirm for stimulating discussions and making experimental results available to us prior to publication. This work was supported by the Deutsche Forschungsgemeinschaft, Sonderforschungsbereich 450 and NATO Cooperative Research Grant No. 974075.

- *Corresponding author: Email: reichling@cup.uni-muenchen.de
- ¹R. T. Williams, M. N. Kabler, W. Hayes, and J. P. Stott, *Phys. Rev. B* **14**, 725 (1976).
- ²A. V. Agafonov and P. A. Rodnyi, *Sov. Phys. Solid State* **25**, 335 (1983).
- ³J. H. Beaumont, W. Hayes, D. L. Kirk, and G. P. Summers, *Proc. R. Soc. London, Ser. A* **315**, 69 (1970).
- ⁴J. Becker, M. Kirm, V. N. Kolobanov, V. N. Makhov, V. V. Mikhailin, A. N. Vasilev, and G. Zimmerer, *Electrochem. Soc. Proc.* **98-25**, 415 (1998).
- ⁵J. Becker, Ph.D. thesis, Universität Hamburg, Germany, 1997, p. 91.
- ⁶E. D. Thoma, H. M. Yochum, and R. T. Williams, *Phys. Rev. B* **56**, 8001 (1997).
- ⁷K. Tanimura and N. Itoh, *Phys. Rev. Lett.* **60**, 2753 (1988).
- ⁸K. Kimura and W. Hong, *Phys. Rev. B* **58**, 6081 (1998).
- ⁹A. Lushchik, E. Feldbach, R. Rink, Ch. Lushchik, M. Kirm, and I. Martinson, *Phys. Rev. B* **53**, 5379 (1996).
- ¹⁰T. Tsujibayashi, M. Watanabe, O. Arimoto, M. Itoh, S. Nakanishi, H. Itoh, S. Asaka, and M. Kamada, *Phys. Rev. B* **60**, R8442 (1999).
- ¹¹The band-gap energies have been extracted from reflectivity spectra presented in G. W. Rubloff, *Phys. Rev. B* **5**, 662 (1972). These values are not in accordance with those given by T. Tomiki and T. Miyata, *J. Phys. Soc. Jpn.* **27**, 658 (1969). Band-gap energies will be discussed in detail elsewhere.
- ¹²P. J. Call, W. Hayes, and M. N. Kabler, *J. Phys. C* **8**, L60 (1975).
- ¹³W. Hayes, R. F. Lambourn, and J. P. Stott, *J. Phys. C* **7**, 2429 (1974).
- ¹⁴S. Parker, K. S. Song, C. R. A. Catlow, and A. M. Stoneham, *J. Phys. C* **14**, 4009 (1981).
- ¹⁵M. N. Kabler and R. T. Williams, *Phys. Rev. B* **18**, 1948 (1978).
- ¹⁶T. Eshita, K. Tanimura, and N. Itoh, *Phys. Status Solidi B* **122**, 489 (1984).
- ¹⁷K. S. Song, C. H. Leung, and J. M. Spaeth, *J. Phys. Condens. Matter* **2**, 6373 (1990).
- ¹⁸C. H. Leung, C. G. Zhang, and K. S. Song, *J. Phys.: Condens. Matter* **4**, 1489 (1992).
- ¹⁹M. Adair, C. H. Leung, and K. S. Song, *J. Phys. C* **18**, L909 (1985).
- ²⁰C. Kittel, *Introduction to Solid State Physics*, 4th ed. (Wiley, New York, 1971), p. 129.
- ²¹R. W. G. Wyckoff, *Crystal Structures*, 2nd ed. (Wiley, New York, 1965), p. 241.
- ²²K. S. Song and C. H. Leung, *J. Phys. Condens. Matter* **1**, 8425 (1989).
- ²³K. S. Song and L. F. Chen, *J. Phys. Soc. Jpn.* **58**, 3022 (1989).